tvst

Article

Quantitative Fundus Autofluorescence in Systemic Chloroquine/Hydroxychloroquine Therapy

Clara Reichel[1,*], Andreas Berlin[1,*], Victoria Radun[1], Ioana-Sandra Tarau[1], Jost Hillenkamp[1], Nikolai Kleefeldt[1], Kenneth R. Sloan[2], and Thomas Ach[1,3]

[1] University Hospital Würzburg, Department of Ophthalmology, Würzburg, Germany
[2] University of Alabama at Birmingham, Department of Ophthalmology, Birmingham, AL, USA
[3] University Hospital Bonn, Department of Ophthalmology, Bonn, Germany

Correspondence: Thomas Ach, MD, FEBO. University Hospital Bonn, Department of Ophthalmology, Ernst Abbe Strasse 2, Bonn, 53127, Germany. e-mail: thomas.ach@ukbonn.de

Received: April 23, 2020
Accepted: August 3, 2020
Published: August 28, 2020

Keywords: quantitative fundus autofluorescence; chloroquine; hydroxychloroquine; bulls eye maculopathy

Citation: Reichel C, Berlin A, Radun V, Tarau I-S, Hillenkamp J, Kleefeldt N, Sloan KR, Ach T. Quantitative fundus autofluorescence in systemic chloroquine/hydroxychloroquine therapy. Trans Vis Sci Tech. 2020;9(9):42, https://doi.org/10.1167/tvst.9.9.42

Purpose: To investigate the effect of systemic chloroquine/hydroxychloroquine (CQ/HCQ) on outer retinal health using quantitative fundus autofluorescence (QAF) imaging.

Methods: For this prospective, cross-sectional study, 44 CQ/HCQ patients and 25 age-matched controls underwent multimodal retinal imaging including QAF (488 nm) and spectral-domain optical coherence tomography (SD-OCT) in addition to the recommended CQ/HCQ screening procedures. Custom written FIJI plugins enabled detailed QAF analysis and correlation with retinal thickness and comparison to the healthy controls.

Results: Out of 44 patients, 29 (mean age 43.5 ± 12.2, range 22–59 years) exposed to CQ/HCQ (mean cumulative dose 724.2 ± 610.4 g, median 608.0 g, range 18.6–2171.0 g) met eligibility criteria. Four of these 29 patients had bull's-eye maculopathy (BEM). Mean QAF values were significantly higher in CQ/HCQ patients than in healthy controls. QAF increase started early after treatment onset, remained high even years after treatment cessation, and was not accompanied by pathologies in the other screening methods, including retinal thicknesses (except in BEM patients).

Conclusions: QAF might be a useful tool in retinal imaging and in verifying systemic CQ/HCQ intake. The early onset and preserved high levels of QAF parallel findings of CQ deposition in the retina in animal models. Whether QAF can be used as a screening tool to detect early CQ/HCQ related maculopathy is the subject of long-term ongoing studies.

Translation Relevance: Experimental QAF imaging in systemic CQ/HCQ therapy monitoring might be a useful tool to indicate the drug or its metabolites and to detect metabolic retinal changes.

Introduction

Chloroquine (CQ) and hydroxychloroquine (HCQ) are effective and widely used systemic drugs to treat several rheumatologic and dermatologic immunologic disorders such as systemic lupus erythematosus or rheumatoid arthritis.[1–3] A well-known complication in long-term, high cumulative dose therapy is the development of a CQ/HCQ-related maculopathy, bearing the possibility of eventually leading to irreversible sight-threatening bull´s eye maculopathy (BEM).[4–6]

Fortunately, the risk of showing CQ/HCQ-related retinal toxicity is very low (<1%) in the first five years of treatment, but it is cumulatively dose-dependent and rises after long-lasting intake.[7] In addition, the increasing use of HCQ (for example, nearly 21,000 newly initiated HCQ therapies in the UK only between 2007 and 2016[8]) implies that the incidence of CQ/HCQ related maculopathies might increase in the near future. If early sings of CQ/HCQ related maculopathies are present, early cessation of medication bears the possibility to stop or even reverse mild pathologic changes and to avoid irreversible vision loss.[9] However, in more

severe cases, maculopathy may worsen even years after CQ/HCQ treatment is stopped.[10–15]

Based on these observations, the American Academy of Ophthalmology (AAO) recommended screening at least at baseline and after 5 years of CQ/HCQ therapy,[16] using structural (spectral-domain optical coherence tomography (SD-OCT) and functional tests (visual acuity, visual field, multifocal electroretinogram).[16,17] In addition, to detect early topographical damage to the outer retina, fundus autofluorescence (FAF) can be qualitatively used.[18,19]

SD-OCT changes, though controversially discussed, include thinning of the inner (ganglion cell layer and inner plexiform layer)[20] or outer retina,[21] or both.[22] FAF alterations, as observed with conventional short wavelength FAF (488 nm excitation), range from increased AF signals in the parafoveal region at early stages[19,23] to a mottled pattern with patchy areas of decreased AF in more advanced stages.[18] These areas of decreased AF will, finally, lead to a loss of RPE and the loss of AF in the parafoveal region with its typical bull's-eye pattern. However, a major limitation of the conventional short wavelength FAF is its restriction to qualitative analyses.

A recent development in FAF imaging is quantitative fundus autofluorescence (QAF), which uses an internal reference for AF intensity normalization. This enables comparison of AF intensities intra- and inter-individually, as well as in long-term follow-up.[24] As for conventional short wavelength FAF, QAF has shown good repeatability[25] and can serve as a diagnostic tool for the healthy and diseased retina, especially in diseases with high potential of FAF alterations in the course of the disease or during treatment.[26–28]

The purpose of this study was to use the experimental QAF technique in addition to the recommended screening tests in patients routinely examined at our department due to systemic CQ/HCQ intake. The QAF signals were analyzed and compared to QAF signals from a healthy age -and sex-matched control group. The results of our preclinical study will promote the debate on QAF as a screening tool in CQ/HCQ treatment monitoring.

Patients and Methods

Study Population

For this monocentric, prospective, cross-sectional study, patients (European Caucasians) with current or past systemic CQ/HCQ intake due to rheumatic disorders were recruited from the Department of Ophthalmology at the University Hospital Würzburg, Germany, between September 2017 and April 2019. All CQ/HCQ patients agreed to participate in this study. Before study entry all patients gave written informed consent after detailed explanation of the nature and consequences of this study. This study was approved by the University of Würzburg Ethics committee (no. 69/17), and all study procedures were performed in compliance with the Declaration of Helsinki.

CQ/HCQ patients were enrolled only if they had clear optic media. Exclusion criteria included presence of retinal diseases (other than CQ/HCQ related maculopathy), unstable fixation, media opacity, or refractive error > 6 Diopters (spherical equivalent).

Twenty-five age- and sex-matched healthy subjects who had routinely planned examination (yearly health check-ups or examination of a diseased fellow-eye) were also recruited at the Department of Ophthalmology, University Hospital Würzburg. These healthy eyes served as controls in the QAF and SD-OCT analysis.

Examinations

At baseline visit, all participants were asked to complete a questionnaire considering height, body weight, and ophthalmologic and general medical history. Furthermore, history of CQ/HCQ exposure was recorded (daily dose and onset and stop date) and cumulative dose was calculated.[29]

Patients were examined following the revised AAO recommendations. This included visual field (12° white-on-white 10-2 automated threshold kinetic perimetry, Octopus; Haag Streit, Bern, Switzerland), multifocal electroretinogram, mfERG (in line with the current ISCEV Standards; CRT monitor, 61 discrete black and white hexagonal pattern[30] stimulation, 27° angle of the posterior pole, centered on the fovea (RETIscan, Version 6.16.3.8; Roland Consult, Brandenburg an der Havel, Germany), color vision testing (HMC anomaloscope; Oculus, Wetzlar, Germany), Farnsworth-Panel D 15 (saturated and unsaturated), macula SD-OCT, and FAF imaging (details for SD-OCT and FAF, see below).

Best corrected visual acuity was determined using the standardized Early Treatment Diabetic Retinopathy Study protocol charts. Comprehensive ophthalmologic examinations included slit lamp biomicroscopy, applanation tonometry, and dilated funduscopy.

Image Acquisition

Before image acquisition, subject's individual c-curves[24] were measured (IOL Master 500; Zeiss, Oberkochen, Germany) and transferred to the Spectralis and modified HRA2 device´s software

(HEYEX; Heidelberg Engineering, Heidelberg, Germany) for proper image size calculation. Pupils were then dilated at a minimum of 6 mm diameter (0.5% tropicamide, 2.5% phenylephrine). Multimodal imaging included SD-OCT (6 mm horizontal macular scan, ART 35 frames, 49 B-scans, 20° × 20°) as well as infrared (IR) and red-free fundus reflectance (30° × 30°), short wavelength FAF (excitation 488 nm, emission 500-750 nm, 30° × 30°), and QAF (excitation 488 nm, emission 500-750 nm, 30° × 30°, 768 × 768 pixels) using a Spectralis and a modified HRA2 device (both Heidelberg Engineering).

QAF Image Acquisition

Details of the QAF technique, modified device´s specifications, as well as QAF image acquisition requirements, have been reported previously.[24,31] Briefly, the modified HRA2 device possesses an internal reference (main fluorophore: solid Texas Red Dye) which is simultaneously excited and recorded during the QAF acquisition process. All captured signal intensities can then be normalized to the signal of this internal reference and differences in laser and camera settings (e.g., laser power or detector sensitivity) are eliminated between individual examinations.

Before QAF imaging, photoreceptors were bleached[24] using the short wavelength light for at least 20 seconds to adequately reduce the absorption of photopigment and to enable reliable QAF signal acquisition. These preparations were immediately followed by the registration of 12 single QAF frames. If necessary, sensitivity of the HRA camera was regulated manually to avoid pixel oversaturation. After checking the quality of each QAF frame, low quality frames (e.g., insufficient illumination, lacking focus on macula, unstable fixation, eye lid interference) were deleted and at least nine image frames were averaged into one final mean QAF image using the manufacturer's software (HEYEX; Heidelberg Engineering, Heidelberg, Germany). In addition, a second identical QAF imaging session with new adjustments of the camera was conducted to ensure repeatability, as previously suggested.[31] We assumed good repeatability if QAF values were within a 15% range. This procedure was then repeated for the fellow eye. Out of these four imaging sessions (two from each eye), the QAF image with the most even illumination across the posterior pole and clearest focus on the central macula was chosen for further analysis. If both eyes had equal quality images, the left eye was chosen.

All QAF images underwent postacquisition adjustments considering reference calibration factor of the device (as delivered by the manufacturer) and the respective age-related optical media of the subject.[32] Finally, the gray value QAF image (scale 0–1200 QAF units), was clipped at 511 because there were few values higher than 511 QAF units. It was then down-scaled to 0–255 for storage as an 8-bit binary image, and then false colored using a color Look Up Table with 256 entries. All QAF images were obtained with the same device and by the same trained operator (CR). Regular device calibration by the manufacturer proofed consistent signal measurements.

SD-OCT Based Multimodal Image Stacks

All images were exported from the image devices and underwent further processing using custom written FIJI (www.fiji.sc[33]) plug-ins, as previously reported (Kleefeldt et al., manuscript in revision, 2019). In brief, each imaging modality was registered against the enface IR image, which was simultaneously captured during the SD-OCT macula scanning. An SD-OCT based multimodal image stack was assembled (Supplementary Fig. S1). For registration, two identical landmarks (e.g., vascular bifurcation) were manually marked in the enface IR image followed by a transformation (limited to translation, rotation, and uniform scaling of the image). To create a specific two-dimensional coordinate system, essential for the QAF analysis, the exact position of the foveola was determined in the macula SD-OCT scan with the foveal dip and the rise of the external limiting membrane. The foveal position could then easily be transferred to the corresponding infrared image (simultaneously acquired during SD-OCT imaging) and subsequently to all other aforementioned images from the multimodal image stack (Supplementary Fig. S1). For better illustration, all eyes were plotted as left eyes.

QAF Analysis

The eight segments of the middle ring of three concentric rings (QAF8) have been widely accepted for QAF intensity analysis.[26,31,34] In a preliminary analysis (data not shown), these QAF8 ring segments did not cover the parafoveal[35,36] atrophic area in the BEM patients (Supplementary Fig. S2). Bisecting each ring segment of the original QAF grid and extending it toward the fovea results in a total of 97 segments (including the foveal area),[37] plus a parafoveal ring (Supplementary Fig. S2). The QAF97 grid uses the fovea (as determined in SD-OCT scan) and the edge of the optic disc (manually marked in the IR images) to define the maximum grid diameter. Therefore ring and

segment dimensions for the QAF97 grid might slightly differ between eyes.

Using custom-written FIJI plugins, the mean, maximum, and minimum QAF values (± standard deviation [STD]), and the number of pixels of the analyzed area for each segment (irrespective of the grid used) were recorded and stored as a tab-delimited text file. The mean value of the 96 extrafoveal segments, the fovea, and the parafovea were used for further statistical analysis in this study.

SD-OCT Based Retinal Thickness Analysis and Correlation with Autofluorescence

Based on the macula SD-OCT scans, retinal thicknesses (whole retina: inner limiting membrane [ILM] to Bruch membrane [BrM]); inner retina: ILM to external limiting membrane (ELM); outer retina: ELM to BrM) were computer-assisted measured at eleven predefined locations (fovea as the center; 0.5 mm steps nasally and temporally) within the horizontal central 6 mm SD-OCT scan using custom written FIJI plugins. These retinal thicknesses were then correlated with QAF values from the corresponding areas at the identical eleven locations within the QAF image (fovea as the center; 0.5 mm steps nasally and temporally; at each sample location, QAF values from pixels in a 5 × 5 grid were averaged).

Statistical Analysis

Data collection, organization, and analysis was performed using SPSS statistic software package (IBM SPSS 25.0; IBM Corporation, Armonk, NY, USA). Categorical variables are presented as numbers and percentages, continuous variables are expressed as means ± STD. $P < 0.05$ was considered statistically significant. Intraclass correlation coefficients were computed to determine the image reading agreement of retinal thickness measurements. Normally distributed continuous variables were tested using quantile-quantile plots, Kolmogorov-Smirnov, and Shapiro-Wilk tests. The Mann-Whitney U-test or *t*-test for independent samples was applied for mean values of all CQ/HCQ patients and controls. An analysis of variation (ANOVA) with Tukey post-hoc analysis was performed for the mean values of the two CQ/HCQ subgroups (patients with/without BEM). More detailed information on statistical tests used can be found in the supplement. The association between age and mean QAF97, as well as cumulative dose and QAF97 was calculated using Spearman's rank correlation coefficient (r_s) or Pearson product-moment correlation (r) coefficient.

Results

Initially, 44 CQ/HCQ patients underwent multimodal imaging. Six patients had to be excluded because of poor image quality. From the remaining 38 patients, an additional nine were excluded because of age greater than 60 years and possible impact of lens AF on total QAF, resulting in 29 patients for final analysis. Demographic data, underlying systemic conditions, and duration of CQ/HCQ treatment are shown in Tables 1 and 2. These patients had no relevant concomitant renal systemic nor previous macular diseases.

Twenty-seven patients were female (93.1%). Mean age of all 29 patients was 43.5 ± 12.2 years (median 45.0 years, range 22–59 years), mean CQ/HCQ cumulative dose was 724 g ± 610 g (median 608.8 g, range 18.6–2171.0 g) with a mean intake duration of 7.5 ± 6.5 years (median 6.9 years, range 0.3–28 years), see Table 2. Four patients (13.8%; mean age 51.8 ± 11.2 years, median 57.0 years, range 35–58 years) showed CQ/HCQ induced maculopathy with abnormalities in all screening modalities (visual fields, mfERG, SD-OCT, and FAF). Best corrected visual acuity in the remaining 25 patients (86.2%, mean age 42.2 ± 12.0 years) was ≥ 20/25 (with only one exception due to amblyopia, best corrected visual acuity 20/40, Table 1).

Patients without CQ/HCQ maculopathy showed no pathologies in 12° perimetry or mfERG, whereas patients with CQ/HCQ maculopathy had scotomas within the 12° visual field and abnormal reduced mfERG amplitudes parafoveally. Color vision tests showed no significant alterations in CQ/HCQ patients.

Twenty-five healthy subjects from our previous study of QAF in healthy subjects served as controls (23 female [92.0%]). Mean age of all controls was 42.0 ± 11.7 years (median 44.0 years, range 23–60 years). A sex- and age-matched subgroup of 10 (mean age 51.8 ± 5.0 years, median 53.0 years, range 45–58 years) out of this healthy cohort served as controls for the CQ/HCQ patients with BEM. Best corrected visual acuity in all controls was ≥ 20/25. All subjects had clear media.

Quantitative Fundus Autofluorescence

In general, in CQ/HCQ patients, QAF values were significantly higher as compared to the age-matched controls (Fig. 1).

Table 1. Demographic Data of CQ/HCQ Patients

Age [years]	Sex	Indication for CQ/HCQ Use	HCQ	CQ	Duration of Intake [years]	Cumulative Dose [g]*	Eye Included	BCVA	BEM
22	F	Sjögren's syndrome	+	–	6.5	402	OD	20/13	–
24	F	Collagenosis	+	–	0.3	24	OS	20/13	–
24	F	Collagenosis	+	–	5.6	693	OS	20/20	–
27	F	RA	+	–	2.5	168	OD	20/16	–
31	F	SLE	+	–	0.3	19	OS	20/20	–
32	F	RA	+	–	1.3	176	OD	20/16	–
33	F	RA	+	–	5.5	401	OS	20/13	–
34	F	SLE	+	–	9.5	754	OS	20/13	–
34	F	SLE	+	–	8.3	608	OS	20/16	–
35	F	SLE	–	+	9.0	867	OD	20/100	+
35	F	SLE	+	–	9.0	912	OS	20/16	–
40	M	SLE	+	–	4.1	365	OS	20/16	–
40	F	SLE	+	–	6.9	511	OS	20/16	–
41	F	SLE	+	–	9.6	1045	OS	20/20	–
45	F	Cutaneous lupus	+	–	2.1	219	OD	20/16	–
45	F	RA	+	–	0.3	36	OD	20/20	–
50	F	RA	–	+	22.0	2007	OS	20/20	–
52	F	SLE	+	–	3.8	511	OS	20/13	–
53	M	RA	+	–	3.8	566	OD	20/13	–
53	F	Cutaneous lupus	+	–	2.6	238	OS	20/16	–
54	F	Lichen ruber planus	+	–	5.5	657	OS	20/16	–
54	F	CREST syndrome	+	+	8.4	635	OD	20/20	–
56	F	SLE	+	+	10.0	1697	OS	20/200	+
57	F	Cutaneous lupus	+	–	13.0	1602	OS	20/16	–
57	F	Sjögren's syndrome	+	–	0.7	45	OD	20/16	–
58	F	RA	–	+	19.0	1733	OS	20/20	+
58	F	Collagenosis	+	+	10.5	2171	OS	20/16	–
58	F	RA	–	+	7.9	730	OD	20/20	+
59	F	SLE	+	+	28.0	1244	OS	20/20	–

M, male; F, female; RA, rheumatoid arthritis; SLE, systemic lupus erythematosus; CREST, calcinosis, Raynaud's phenomenon, esophageal dysmotility, sclerodactyly, and telangiectasia; BCVA, best corrected visual acuity (Early Treatment Diabetic Retinopathy Study charts in 4 meters distance); OD, os dexter; OS, os sinister.

*Cumulative dose of CQ and HCQ in sum.

Mean QAF97 intensity was 285.2 ± 72.0 [QAF a.u.] in all CQ/HCQ patients ($P = 0.015$), 278.1 ± 72.6 [QAF arbitrary units (a.u.)] in CQ/HCQ patients without BEM ($P = 0.045$), and 329.5 ± 56.5 [QAF a.u.] in patients with BEM ($P = 0.228$), respectively. In all healthy controls, mean QAF97 was 235.4 ± 73.8 [QAF a.u.], while in the matched group for CQ/HCQ patients with BEM mean QAF97 was 283.0 ± 64.5 [QAF a.u.].

Table 2. Characteristics of CQ/HCQ Patients and Healthy Controls

Demographic Characteristics and Mean QAF97 Values in CQ/HCQ Patients and Healthy Controls				
Parameter	CQ/HCQ	Controls	Significance Level [*t*-Test]	Significance Level [ANOVA with Tukey Post hoc Test]
N	29	25		
Females, n (%)	27 (93.1)	23 (92.0)		
N	29	25		
Without BEM, n (%)	25 (86.2)	23 (92.0)		
N	4	10		
With BEM, n (%)	4 (13.8)	10 (40.0)		
Mean age, years				
All	43.5 ± 12.2	42.0 ± 11.7	$P = 0.642$	
Range	22–59	23–60		
Without BEM	42.2 ± 12.0	42.0 ± 11.7	$P = 0.998$	
Range	22–59	23–60		
With BEM	51.8 ± 11.2	51.8 ± 5.0	$P = 0.954$	
Range	35–58	45–58		
Mean QAF97 [QAF a.u.]				
All	285.2 ± 72.0	235.4 ± 73.8	$P = 0.015$	
Range	150.0–478.6	92.1–368.1		
Without BEM	278.1 ± 72.6	235.4 ± 73.8	$P = 0.045$	$P = 0.143$
Range	150.0–478.6	92.1–368.1		
With BEM	329.5 ± 56.5	283.0 ± 64.5	$P = 0.228$	$P = 0.277$
Range	260.4–390.9	158.6–358.1		
Mean intake duration, years				
All	7.5 ± 6.5			
Median	6.9			
Range	0.3–28			
Without BEM	6.9 ± 6.6			
Range	0.3–28			
With BEM	11.2 ± 5.1			
Range	8–19			
Mean cumulative dose, g				
All	724.2 ± 610.4			
Median	608.0			
Range	18.6–2171.0			
Without BEM	639.0 ± 586.9			
Range	18.6–2171.0			
With BEM	1256.8 ± 532.3			
Range	730.0–1733.0			

Where applicable, values are presented as means ± standard deviation.

In all subjects (patients and controls), mean QAF intensities significantly increased with age (all CQ/HCQ patients: r = 0.6, $P < 0.001$; patients without BEM: r = 0.6, $P = 0.001$; patients with BEM: r = 0.8, $P = 0.132$; healthy controls: r = 0.6, $P = 0.001$; Fig. 1) until age 60. Despite the generally increased FAF in CQ/HCQ patients, FAF distribution across the posterior pole is similar as in functional and structural

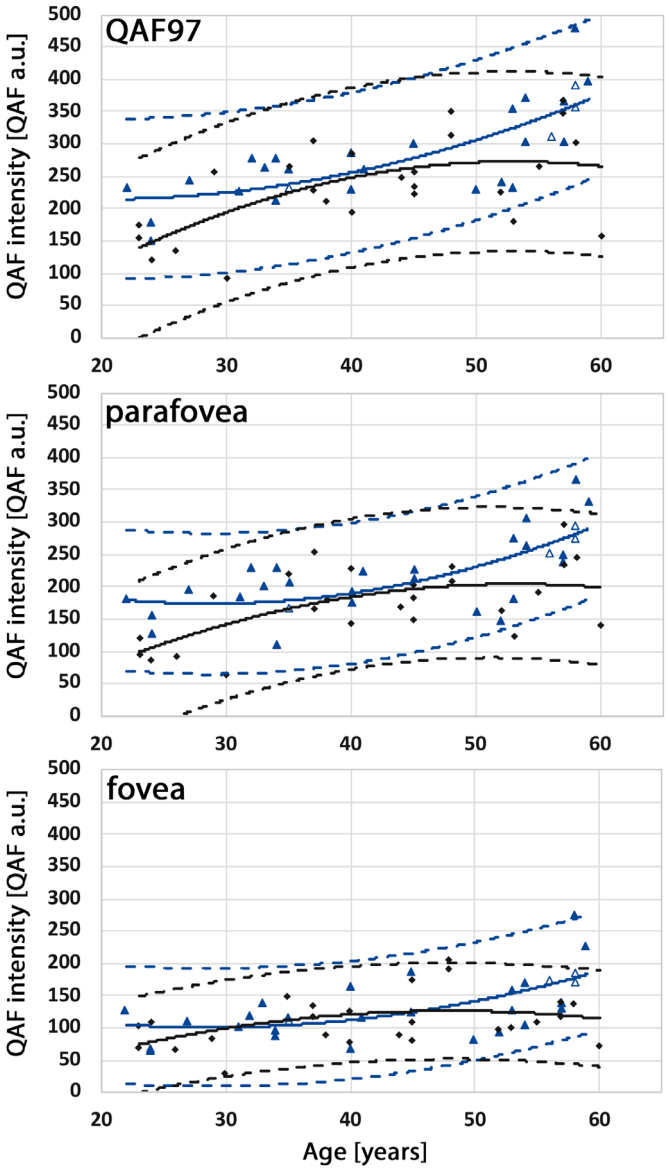

Figure 1. Quantitative fundus autofluorescence in CQ/HCQ patients. In patients with CQ/HCQ intake (*blue filled and transparent triangles*), QAF values are significantly higher as compared with age-matched controls (*black dots*). Patients with CQ/HCQ related maculopathy (*blue transparent triangles*) were older and had higher QAF values as compared with patients without maculopathy (*blue filled triangles*). The overall trend of increasing QAF with aging is visible in all study subjects (patients and controls). The QAF at the fovea (segment "f" in QAF97 [Supplementary Figure S2]) is low (due to light blocking macular pigment and low number of lipofuscin granules compared to parafovea) but at same levels for CQ/HCQ patients and controls. The QAF at the parafovea (segment "pf" in QAF97 [Supplementary Figure S2]) follows the trend of increased QAF in CQ/HCQ patients, even in patients with BEM (*blue transparent triangles*). Shown are individual QAF values from all CQ/HCQ patients and healthy controls (*black rhombi*), as well as mean (*lines*) and 95% confidence intervals (*dashed lines*); *blue*: CQ/HCQ patients, *black*: healthy controls.

healthy controls, showing increased AF intensities at the parafovea and a maximum temporal-superior (Figs. 2A, 2B).

If the whole group and the different phenotypes (BEM present: yes/no) were taken into account, an ANOVA test revealed significant differences between CQ/HCQ patients with/without BEM and controls ($P = 0.015$). Tukey's post-hoc analysis showed neither a significant difference for QAF97 between controls and CQ/HCQ patients with BEM ($P = 0.143$), although there was no significant difference between controls and CQ/HCQ patients without BEM ($P = 0.277$).

Interestingly, in patients with bull´s eye maculopathy, QAF remains high even years (5-12 years) after drug cessation (Figs. 2C–2E). The highest QAF values can be found at the superior-temporal region in patients without maculopathy (Fig. 3). In patients with BEM, there is slight rotation with the highest QAF values preferable at the temporal macula.

QAF and Cumulative Dose/Duration of Intake

There was no significant difference ($P = 0.136$) in QAF97 intensities between patients with cumulative dose <1000 g and patients with cumulative dose >1000 g. In general, higher cumulative dose did not lead to higher QAF (Fig. 4). Also, there was no significant difference between QAF intensities for CQ/HCQ intake more or less than five years ($P = 0.540$). However, it is noticeable that even in patients with short CQ/HCQ treatment duration of a few months (in our study around four months) increased QAF intensities are detectable (Fig. 4).

Correlation of Retinal Thicknesses and Autofluorescence

Patients with BEM showed significant thinner retina at all eleven measured points (whole retina, inner retina, outer retina) using the custom written FIJI plugin, compared to patients without BEM and healthy controls (Fig. 5, Supplementary Table S1). Three BEM patients presented preserved central fovea ("flying saucer" sign[38]) but parafoveal loss of outer retinal layers, whereas two subjects with advanced BEM also had central retinal atrophy (Figs. 2C–2E, Supplementary Fig. S2).

Patients without BEM showed significant thicker retina at the fovea as compared to controls using the custom FIJI plugin (measurement points 0 [whole retina, WR - inner retina, IR] and −0.5, +0.5 mm (IR) (Fig. 5, Supplementary Table S1). In patients

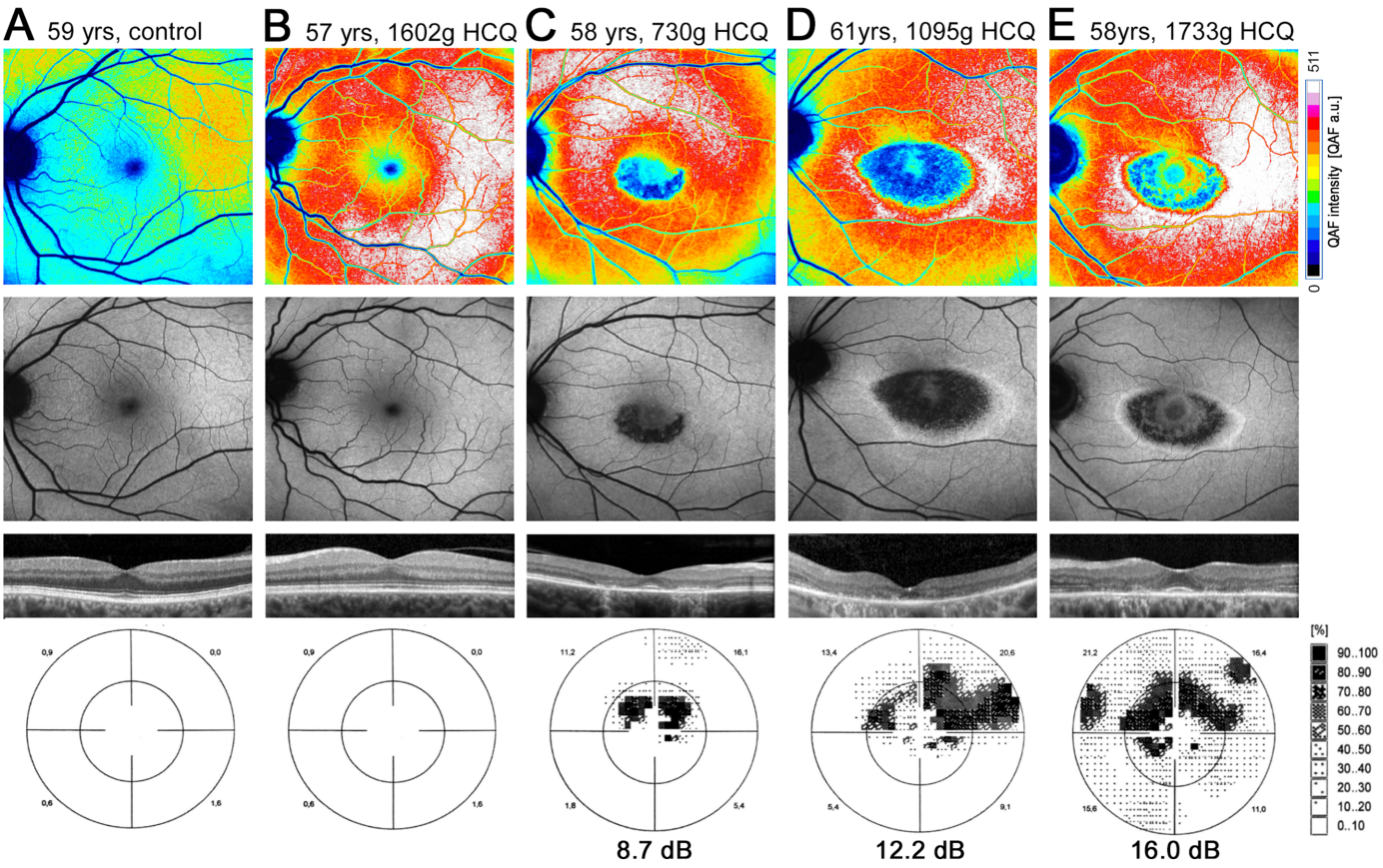

Figure 2. High QAF levels in CQ/HCQ and structural/functional alterations. In a functional and structural healthy control (A), QAF shows normal intensities across the posterior pole with highest values at the temporal-superior region. CQ/HCQ (B–E) patients have significantly increased QAF intensities throughout the posterior pole. Interestingly, the increased QAF is not necessarily correlated with structural or functional alterations (B). In contrast, patients with BEM have the same high levels of QAF but with structural (SD-OCT) and corresponding functional (autofluorescence (AF), perimetry) alterations (C–E). Of note, in patients with BEM, QAF intensity remains high even years after cessation of the medication: 5 years (C), 12 years (D), 5 years (E) after drug cessation. The scotomas in the visual fields are reported as deviation [dB] from the normal (0 dB).

with or without BEM, focal measurements at the 11 points revealed no significant correlations (Supplementary Table S2).

Discussion

This study evaluated the usefulness of QAF in the screening process of patients using systemic CQ/HCQ medication. Our results demonstrate increased QAF values in patients with or without BEM, as compared to age- and sex-matched controls. The increased QAF values are only minimally correlated with retinal thickness. QAF can be used as a biomarker for CQ/HCQ intake; however, our presented data does not proof QAF as a screening tool for CQ/HCQ maculopathy at this time. Furthermore, QAF analysis in CQ/HCQ patients requires adjustable analysis tools because CQ/HCQ-related lesions are beyond the common QAF analysis grids.

CQ/HCQ related maculopathy is a well-known complication in systemic CQ/HCQ therapy, which could affect up to 20% of all patients after 20 years of intake. There is a continuing trend of increasing prescriptions and also re-evaluating CQ/HCQ for new therapeutic indications such as anti-infectious disease and adjunct antineoplastic therapy or application in diabetes mellitus and heart disease.[1,39] Only recently, the use of chloroquine is intensively discussed as a treatment option in COVID-19 disease,[40] and numerous studies are ongoing or in preparation examining the protective effect of hydroxychloroquine in corona virus disease.[41] This means that an even larger patient population might be exposed to CQ/HCQ in the future and, if intake is long enough, at risk for potential retinal toxicity and sight-threatening maculopathy, especially if concomitant pathologic conditions are present.[16]

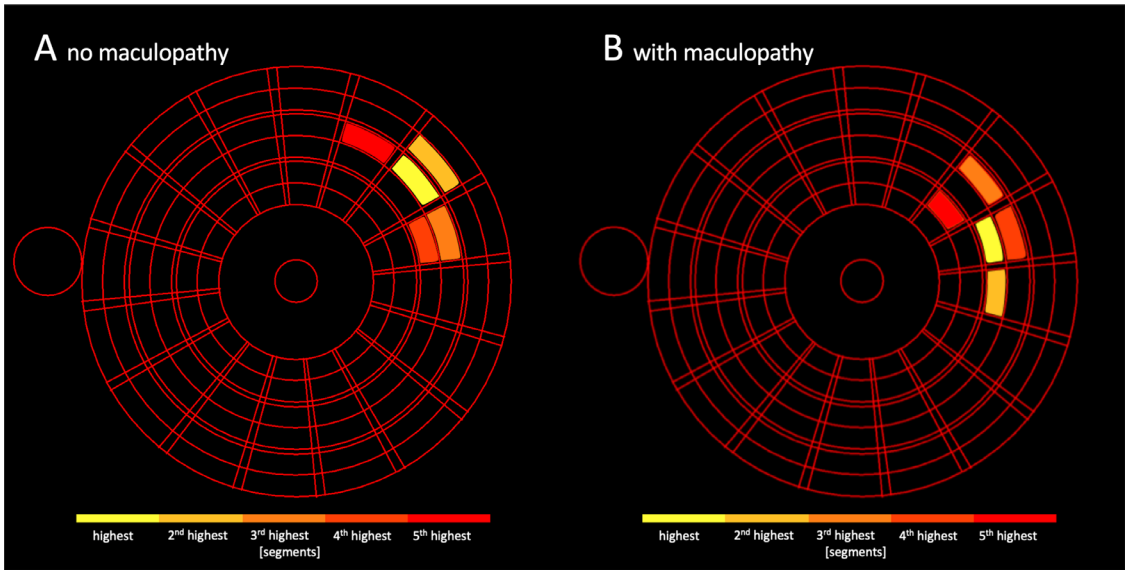

Figure 3. Segments with highest QAF values. Plotted are the five segments with the highest QAF values. Patients without maculopathy (A) show highest segments in the temporal/temporal-superior region. In patients with maculopathy (B), there is a slight rotation of the highest segments towards the temporal region.

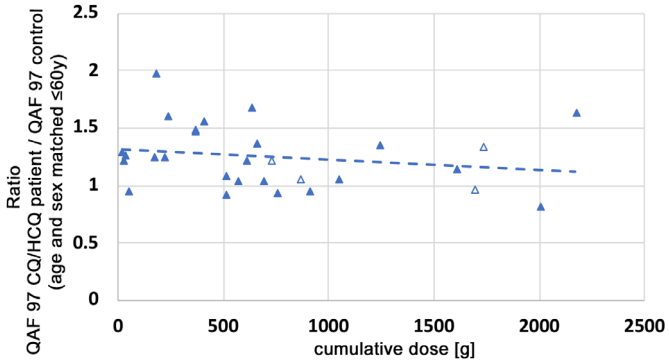

Figure 4. QAF and cumulative dose. Increased QAF intensities seem not to be related to cumulative doses. The graph shows the relation between QAF97 of CQ/HCQ patients versus QAF97 of age-matched controls. A QAF ratio of 1.0 means that QAF97 from a CQ/HCQ patient is identical to the mean QAF97 from at least three age (± 2 years) and sex matched controls. Higher cumulative dose does not lead to further increasing QAF intensities. The plots also show the mean (*blue line*) and the 95% confidence interval (*blue dashed lines*), CQ/HCQ patients without (*blue filled triangles*) and with (*blue transparent triangles*) BEM.

The importance of continuing ophthalmic examinations and maculopathy screening has been discussed extensively and is well accepted nowadays.[42,43] In real life, however, not all CQ/HCQ patients have access to or are even aware of the necessary of retinal screening.

In the revised 2016 version of recommendations on screening for chloroquine and hydroxychloroquine retinopathy the AAO recommends the use of several tests in the screening of CQ/HCQ patients, including structural and functional tests.[16] Although there is still debate about which screening tool is the best to detect CQ/HCQ related maculopathy,[44] FAF has been considered being sensitive enough to detect those changes.[16,18,19]

Within the last years, FAF analysis methods have markedly improved, and FAF imaging is far beyond sole qualitative analysis. Delori and coworkers[24] introduced a modified FAF camera in 2011, which has an internal well-defined fluorescent probe to quantify FAF signal. This probe emits light that is simultaneously captured during regular fundus autofluorescence imaging and serves as the basis for quantification of FAF intensities. The use[26,27,34] and repeatability of QAF[24,31,45] has successfully been demonstrated in several hereditary and degenerative retinal disease studies. The significantly increased QAF signals in CQ/HCQ patients leaves room for debate.

Our proposed hypothesis is that the drug itself or its metabolic by-products are autofluorescent[46] and stored within retinal cells or adjacent tissue, supported in several ways by findings in animal models. First, early studies found that chloroquine deposition is related to pigmented tissue (iris, RPE, choroid), although absent in nonpigmented tissue and albino animals.[47–49] This finding has been confirmed in rhesus monkeys.[50] The retinal drug deposition (probably at the RPE level, see above) is supported by the finding of generally increased QAF intensities in CQ/HCQ patients, still

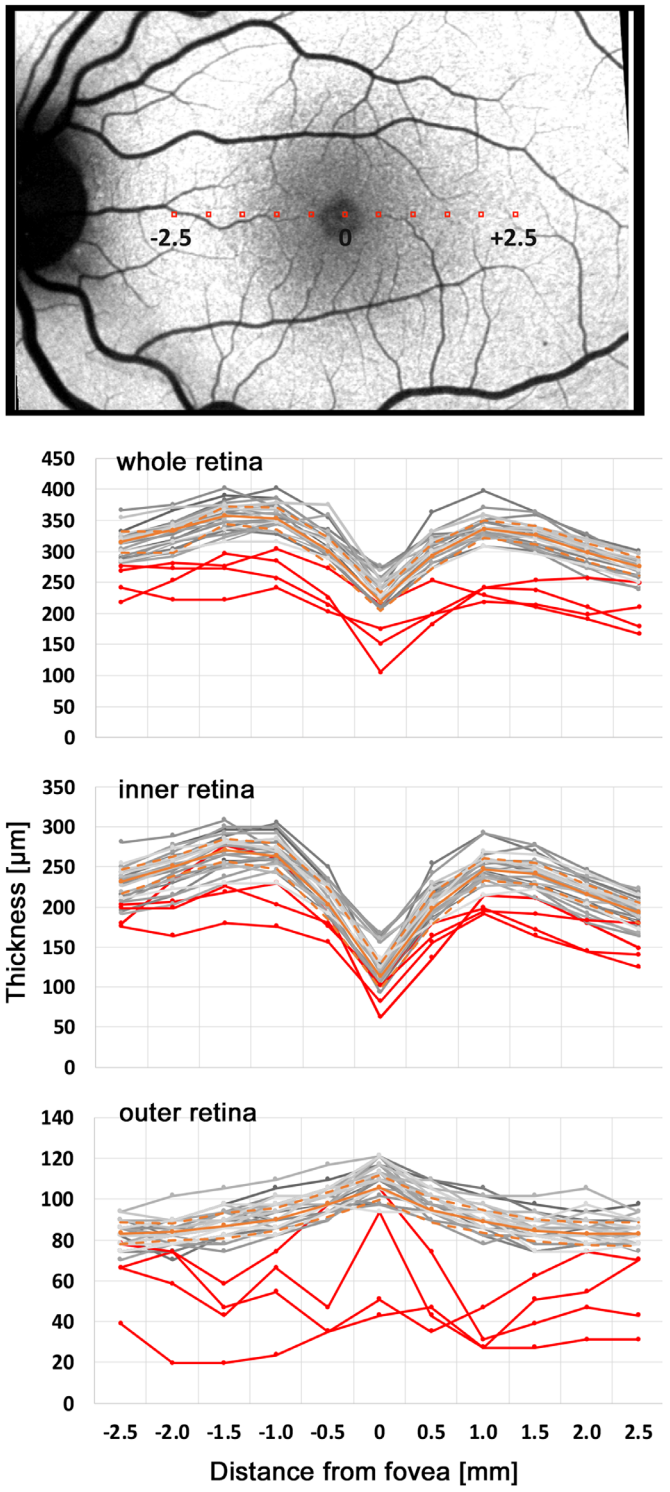

Figure 5. QAF and retina structure. Mean QAF intensities (5 × 5 pixels) and retinal thicknesses (focal measurements in the corresponding foveal SD-OCT scan) were measured and correlated at 11 points (−2.5 mm nasally to +2.5 mm temporally; 0.5 mm distance; centered on the fovea) across a horizontal line. For CQ/HCQ patients without bull´s eye maculopathy, the increased QAF at the posterior pole is not related to measurable layer thickness changes (whole retina, inner and outer retina) outside the foveola, as determined in SD-OCT and compared to healthy controls (orange line). However, in this patient group (CQ/HCQ patients with no signs of bull´s eye maculopathy), the fovea was thicker as compared to controls. Correlation of QAF and retinal thicknesses revealed no significant results (Supplementary Table S2). In patients with BEM (*red lines*), retinal thicknesses (whole retina, inner/outer retina) are significantly reduced compared to controls and CQ/HCQ patients without bull´s eye maculopathy. Whole retina (internal limiting membrane [ILM] to retinal pigment epithelium [RPE]); inner retina (ILM-ELM); outer retina (ELM-RPE). Healthy controls (mean: *orange line*; 95% confidence interval: *dotted orange line*), CQ/HCQ patients (individual patient: *gray line*), BEM patients (*red line*).

maintaining the typical FAF pattern (high parafoveal AF and less AF at the fovea). Second, the long-term effect of CQ/HCQ traceability: in animals, the drug levels in the retina were high even years after cessation, while absent in other tissues of the body.[47,51] This result is in line with increased QAF in our patients with high levels of QAF even more than five years and up to at least 12 years after termination of CQ/HCQ use (see Figs. 2C–2E). Furthermore, the early onset of increased QAF (in our study about six months after treatment start) is also supported by animal models showing high retinal chloroquine levels immediately after drug administration and drug traceability even weeks after a single injection.[47] Bernstein et al.[47] summarized these findings in animals as "extensive [retinal] tissue accumulation and prolonged retention"—a model probably transferrable to the human retina and now trackable with QAF. QAF increase and persistent high QAF levels not related to the duration of intake and cumulative dose would also support these findings.

Other explanations for increased QAF levels include changes in lipofuscin, an age-related rather than toxic granule,[52] within the retinal pigment epithelium.[53] Lipofuscin granules comprise a variety of mostly unknown fluorophores that possess spectral emission features[54] and accumulate with age in healthy RPE cells,[55] clinically confirmed in several QAF studies.[24,31] This age effect of increasing QAF is also detectable in our study cohort, both in patients and controls. Also, the AF distribution pattern across the posterior pole (highest autofluorescence at the parafovea[24,31]) in CQ/HCQ patients is similar to the healthy controls. Increased fundus QAF levels have been observed in some hereditary retinal diseases,[26,27] but none of our patients had any history or clinical signs of hereditary retinopathy.

The increased QAF levels in CQ/HCQ patients could also reflect increased metabolic activity in the photoreceptor/RPE system, enforced by the drug or its metabolites. RPE cells are in close interaction with both cones and rods (shedding and diges-

tion of photoreceptor outer segments, accumulation of nondegradable lipofuscin).[56,57] Whereas the normal FAF distribution follows the rods rather the cones,[58,59] although cones also contribute to the total FAF signal, the overall increased QAF levels at the whole posterior pole in CQ/HCQ patients suggests that both the rod and cone system is affected. The continued use of drugs such as CQ/HCQ might have toxic effects on photoreceptors and lead to a shortening of photoreceptor outer segments resulting in increased autofluorescence from the RPE[60] as speculated for flood plain hyperautofluorescence in neovascular age-related macular degeneration.[61] However, our structural SD-OCT did not reveal any significant thinning of the outer retina (except: patients with existing BEM nor show any correlation between autofluorescence increase and retinal thickness in all eyes without BEM.

The rationale behind the fact that photoreceptors and RPE at the parafovea are clinically and histologically most affected by the toxic effects of CQ/HCQ and whether RPE or photoreceptors are the primary site of degeneration remains unclear. The multimodal detectable[62–65] CQ/HCQ maculopathy pattern that normally starts at the parafovea might be somehow related to the photoreceptor distribution with highest rod density 3 to 5 mm outside the fovea.[66]

Of note, the increased QAF intensities in our patients without BEM was not accompanied by obvious pathologies in any of the AAO recommended functional and structural screening tests. Neither common 488 nm FAF, visual fields, color vision, electrophysiology, or SD-OCT scans revealed any abnormalities. Furthermore, there was no obvious correlation between increased QAF intensities and retinal thicknesses in our patient cohort (exception: patients with BEM), as determined in QAF measurements and parallel SD-OCT scans.

SD-OCT is considered to be an important screening and classification tool in the management of CQ/HCQ induced maculopathy[16,17] and several groups showed thinning of outer nuclear layer, loss of inner segment/outer segment junctions, as well as loss of RPE.[23,38,67,68] These changes can progress even years after cessation of the medication.[21,64] In our non-BEM patients, there was no obvious general reduction in retinal layer thickness measurable (selective measurements at eleven points across a horizontal line at the posterior pole), in line with other studies.[68] In addition, changes in SD-OCT reflectivity at the parafoveal ellipsoid zone and loss of a continuous interdigitation zone[69] and increased reflectivity in the outer nuclear layer[63] might be early signs of maculopathy and precede findings in any of the other screening modalities. Loss of reflectivity at the photoreceptor level could lead to decreased light-blocking phenomena of photoreceptor pigment and consequently to an increase of the FAF signal. However, because the aforementioned described SD-OCT changes are restricted to the parafovea, this SD-OCT finding doesn´t explain ubiquitous increased QAF at the posterior pole.

Emerging FAF imaging techniques like fluorescence lifetime imaging ophthalmoscopy (FLIO) might definitely add to QAF in screening for CQ/HCQ induced maculopathy. Recently, several groups reported prolonged lifetimes at the parafoveal region in patients with HCQ retinal toxicity.[46,70] However, whether FLIO could be a screening tool for early detection of CQ/HCQ induced maculopathy is still controversially discussed.[46,70]

So far, in QAF studies, QAF8 (eight segments from a projected analysis grid, centered on the fovea, as introduced by Greenberg et al.[31]) was used for analysis. As shown in our study, especially in the maculopathy patients, QAF8 analysis does not capture the affected areas and more flexible analysis patterns (narrowing of the analysis field, flexible dimensions, free hand tools) are warranted to specifically analyze the respective areas.[37,71]

Limitations of this study include an imbalance according to gender, which is due to prevalence and incidence of the rheumatologic disorders and CQ/HCQ drug indications. Furthermore, cumulative dose and intake duration are mostly based on patient recall and were only partially available from documented patient charts, which might have led to unprecise cumulative doses in patients with long-lasting intake. Also, number of patients with drug induced maculopathy are not equally distributed due to limited recruitment possibilities. Documentation regarding macula status before the start of CQ/HCQ treatment was not available for all patients. However, our documentation (history, available images) for the five CQ/HCQ maculopathy patients revealed no signs of maculopathy based on causes other than CQ/HCQ (i.e., no history or signs of hereditary retinal disease, no signs of age-related macular degeneration). Because of the technical limitations of the device only the QAF features of the posterior pole have been examined and it is not clear whether QAF in the periphery or at the ora serrata would show similar results. Finally, our healthy control group did not have any signs of systemic rheumatologic disorders, which could per se (without any CQ/HCQ treatment) lead to increased QAF levels. In a few patients whom we examined before CQ/HCQ treatment start, QAF levels were comparable to the healthy controls (data not shown).

QAF is still in the experimental stage and depends on good imaging conditions, with clear optic media

being the most important one. Therefore QAF values from phakic patients over 60 years (although biomicroscopically clear lens) should be critically reviewed. However, including subjects over age 60 years led to significant QAF differences between the patients without maculopathy and controls, probably because of a physiological QAF decline in normal aging whereas QAF in CQ/HCQ patients remained high (data not shown). Furthermore, well-trained technical assistance is required to guarantee reliability and repeatability of QAF imaging. Previous studies in our cohorts showed mean variability of about 8% in normal subjects[37] and <12% in patients with maculopathy, comparable to results from other groups.[31]

In conclusion, this study is a prospective preclinical report on increased quantitative short wavelength FAF during CQ/HCQ treatment, compared to QAF of healthy controls. Although SD-OCT might be useful in detection of early maculopathy, QAF proves its clinical benefit in CQ/HCQ screening as the first tool that might indicate CQ/HCQ intake in general. Whether increased QAF in CQ/HCQ patients imperatively results in higher risk for the development of outer retinal atrophy or BEM needs further evaluation in larger cohorts and long-term follow-up studies, which are currently recruiting.

Acknowledgments

Supported NIH/NEI 1R01EY027948 (TA); Heidelberg Engineering provided the modified hardware for QAF imaging and technical support.

Parts of this work have been presented at ARVO 2019, Vancouver, Canada; DOG 2019, Berlin, Germany; and the Macula Society 2020, San Diego, USA.

Disclosure: **C. Reichel,** None; **A. Berlin,** None; **V. Radun,** None; **I.-S. Tarau,** None; **J. Hillenkamp,** None; **N. Kleefeldt,** None; **K.R. Sloan,** MacRegen (I); **T. Ach,** Novartis (F, R), Roche (C), MacRegen (I)

* CR and AB contributed equally to this work and should be considered co-first authors.

References

1. Plantone D, Koudriavtseva T. Current and future use of chloroquine and hydroxychloroquine in infectious, immune, neoplastic, and neurological diseases: a mini-review. *Clin Drug Investig*. 2018;38:653–671.
2. Shipman WD, Vernice NA, Demetres M, Jorizzo JL. An update on the use of hydroxychloroquine in cutaneous lupus erythematosus: a systematic review. *J Am Acad Dermatol*. 2020;82:709–722.
3. Rempenault C, Combe B, Barnetche T, et al. Metabolic and cardiovascular benefits of hydroxychloroquine in patients with rheumatoid arthritis: a systematic review and meta-analysis. *Ann Rheum Dis*. 2018;77:98–103.
4. Mavrikakis I, Sfikakis PP, Mavrikakis E, et al. The incidence of irreversible retinal toxicity in patients treated with hydroxychloroquine: a reappraisal. *Ophthalmology*. 2003;110:1321–1326.
5. Browning DJ. Hydroxychloroquine and chloroquine retinopathy: screening for drug toxicity. *Am J Ophthalmol*. 2002;133:649–656.
6. Costedoat-Chalumeau N, Dunogue B, Leroux G, et al. A critical review of the effects of hydroxychloroquine and chloroquine on the eye. *Clin Rev Allergy Immunol*. 2015;49:317–326.
7. Melles RB, Marmor MF. The risk of toxic retinopathy in patients on long-term hydroxychloroquine therapy. *JAMA Ophthalmol*. 2014;132:1453–1460.
8. Jorge AM, Melles RB, Zhang Y, et al. Hydroxychloroquine prescription trends and predictors for excess dosing per recent ophthalmology guidelines. *Arthritis Res Ther*. 2018;20:133.
9. Percival S, Meanock I. Chloroquine: ophthalmological safety, and clinical assessment in rheumatoid arthritis. *Br Med J*. 1968;3:579–584.
10. Sassani J, Brucker A, Cobbs W, Campbell C. Progressive chloroquine retinopathy. *Ann Ophthalmol*. 1983;15:19–22.
11. Kazi MS, Saurabh K, Rishi P, Rishi E. Delayed onset chloroquine retinopathy presenting 10 years after long-term usage of chloroquine. *Middle East Afr J Ophthalmol*. 2013;20:89–91.
12. Ehrenfeld M, Nesher R, Merin S. Delayed-onset chloroquine retinopathy. *Br J Ophthalmol*. 1986;70:281–283.
13. Brinkley JR, Dubois EL, Ryan SJ. Long-term course of chloroquine retinopathy after cessation of medication. *Am J Ophthalmol*. 1979;88:1–11.
14. Carr RE, Henkind P, Rothfield N, Siegel IM. Ocular toxicity of antimalarial drugs: long-term follow-up. *Am J Ophthalmol*. 1968;66:738–744.
15. Ogawa S, Kurumatani N, Shibaike N, Yamazoe S. Progression of retinopathy long after cessation of chloroquine therapy. *Lancet*. 1979;313:1408.

16. Marmor MF, Kellner U, Lai TY, Melles RB, Mieler WF. Recommendations on screening for chloroquine and hydroxychloroquine retinopathy (2016 revision). *Ophthalmology*. 2016;123:1386–1394.
17. Cukras C, Huynh N, Vitale S, Wong WT, Ferris FL, 3rd Sieving PA. Subjective and objective screening tests for hydroxychloroquine toxicity. *Ophthalmology*. 2015;122:356–366.
18. Kellner U, Kellner S, Weinitz S. Chloroquine retinopathy: lipofuscin-and melanin-related fundus autofluorescence, optical coherence tomography and multifocal electroretinography. *Doc Ophthalmol*. 2008;116:119–127.
19. Kellner U, Renner AB, Tillack H. Fundus autofluorescence and mfERG for early detection of retinal alterations in patients using chloroquine/hydroxychloroquine. *Invest Ophthalmol Vis Sci*. 2006;47:3531–3538.
20. Pasadhika S, Fishman G. Effects of chronic exposure to hydroxychloroquine or chloroquine on inner retinal structures. *Eye*. 2010;24:340–346.
21. de Sisternes L, Hu J, Rubin DL, Marmor MF. Localization of damage in progressive hydroxychloroquine retinopathy on and off the drug: inner versus outer retina, parafovea versus peripheral fovea. *Invest Ophthalmol Vis Sci*. 2015;56:3415–3426.
22. Lally DR, Heier JS, Baumal C, et al. Expanded spectral domain-OCT findings in the early detection of hydroxychloroquine retinopathy and changes following drug cessation. *Int J Retina Vitreous*. 2016;2:18.
23. Kellner S, Weinitz S, Kellner U. Spectral domain optical coherence tomography detects early stages of chloroquine retinopathy similar to multifocal electroretinography, fundus autofluorescence and near-infrared autofluorescence. *Br J Ophthalmol*. 2009;93:1444–1447.
24. Delori F, Greenberg JP, Woods RL, et al. Quantitative measurements of autofluorescence with the scanning laser ophthalmoscope. *Invest Ophthalmol Vis Sci*. 2011;52:9379–9390.
25. Reiter GS, Told R, Baratsits M, et al. Repeatability and reliability of quantitative fundus autofluorescence imaging in patients with early and intermediate age-related macular degeneration. *Acta Ophthalmol (Copenh)*. 2019;97:e526–e532.
26. Burke TR, Duncker T, Woods RL, et al. Quantitative Fundus Autofluorescence in Recessive Stargardt DiseaseAutofluorescence in Stargardt Disease. *Invest Ophthalmol Vis Sci*. 2014;55:2841–2852.
27. Duncker T, Tsang SH, Lee W, et al. Quantitative fundus autofluorescence distinguishes ABCA4-associated and non-ABCA4-associated bull's-eye Maculopathy. *Ophthalmology*. 2015;122:345–355.
28. Duncker T, Greenberg JP, Ramachandran R, et al. Quantitative fundus autofluorescence and optical coherence tomography in best vitelliform macular dystrophy. *Invest Ophthalmol Vis Sci*. 2014;55:1471–1482.
29. Plaquenil risk calculators. Available at: https://www.eyedock.com/plaquenil-calcs. Accessed December 29, 2019.
30. Hood DC, Bach M, Brigell M, et al. ISCEV standard for clinical multifocal electroretinography (mfERG)(2011 edition). *Doc Ophthalmol*. 2012;124:1–13.
31. Greenberg JP, Duncker T, Woods RL, Smith RT, Sparrow JR, Delori FC. Quantitative fundus autofluorescence in healthy eyes. *Invest Ophthalmol Vis Sci*. 2013;54:5684–5693.
32. Van De Kraats J, Van Norren D. Optical density of the aging human ocular media in the visible and the UV. *JOSA A*. 2007;24:1842–1857.
33. Schindelin J, Arganda-Carreras I, Frise E, et al. Fiji: an open-source platform for biological-image analysis. *Nature Methods*. 2012;9:676–682.
34. Gliem M, Müller PL, Finger RP, McGuinness MB, Holz FG, Issa PC. Quantitative fundus autofluorescence in early and intermediate age-related macular degeneration. *JAMA Ophthalmol*. 2016;134:817–824.
35. Polyak SL. *The Retina: The Anatomy and the Histology of the Retina In Man Ape, and Monkey, Including the Consideration of Visual Functions, the History of Physiological Optics, and the Histological Laboratory Technique*. 1st ed. Chicago, IL, University of Chicago Press, 1941.
36. Quinn N, Csincsik L, Flynn E, et al. The clinical relevance of visualising the peripheral retina. *Prog Retin Eye Res*. 2019;68:83–109.
37. Kleefeldt N, Tarau IS, Hillenkamp J, Berlin A, Sloan KR, Ach T. Quantitative fundus autofluorescence: advanced analysis tools. *Translational Vis Sci Technol*. 2020;9:2.
38. Brown DM, s Benz M, Wong TP, Major JC. Spectral domain optical coherence tomography as an effective screening test for hydroxychloroquine retinopathy (the "flying saucer" sign). *Clin Ophthalmol*. 2010;4:1151–1158.
39. Shippey E, Wagler VD, Collamer AN. Hydroxychloroquine: an old drug with new relevance. *Cleve Clin J Med*. 2018;85:459–467.

40. Gao J, Tian Z, Yang X. Breakthrough: Chloroquine phosphate has shown apparent efficacy in treatment of COVID-19 associated pneumonia in clinical studies. *Biosci Trends*. 2020;14:72–73.
41. Cortegiani A, Ingoglia G, Ippolito M, Giarratano A, Einav S. A systematic review on the efficacy and safety of chloroquine for the treatment of COVID-19. *J Crit Care*. 2020;57:279–283.
42. Brandao LM, Palmowski-Wolfe AM. A possible early sign of hydroxychloroquine macular toxicity. *Doc Ophthalmol*. 2016;132:75–81.
43. Browning DJ. The prevalence of hydroxychloroquine retinopathy and toxic dosing, and the role of the ophthalmologist in reducing both. *Am J Ophthalmol*. 2016;166:ix–xi.
44. Cukras CA. Screening for hydroxychloroquine retinopathy—can we do better? *LWW*. 2019;39:423–425.
45. Smith R, Greenberg J, Delori F. Quantitative Autofluorescence Measurements. *Acta Ophthalmol (Copenh)*. 2011;89.
46. Sauer L, Calvo CM, Vitale AS, Henrie N, Milliken CM, Bernstein PS. Imaging of hydroxychloroquine toxicity with fluorescence lifetime imaging ophthalmoscopy (FLIO). *Ophthalmology Retina*. 2019;3:814–825.
47. Bernstein H, Zvaifler N, Rubin M, Mansour AM. The ocular deposition of chloroquine. *Invest Ophthalmol Vis Sci*. 1963;2:384–392.
48. McChesney EW, Banks Jr WF, Sullivan DJ. Metabolism of chloroquine and hydroxychloroquine in albino and pigmented rats. *Toxicol Appl Pharmacol*. 1965;7:627–636.
49. Gleiser CA, Dukes TW, Lawwill T, Read WK, Bay WW, Brown RS. Ocular changes in swine associated with chloroquine toxicity. *Am J Ophthalmol*. 1969;67:399–405.
50. Rosenthal A, Kolb H, Bergsma D, Huxsoll D, Hopkins J. Chloroquine retinopathy in the rhesus monkey. *Invest Ophthalmol Vis Sci*. 1978;17:1158–1175.
51. Rubin M, Bernstein HN, Zvaifler NJ. Studies on the pharmacology of chloroquine: Recommendations for the treatment of chloroquine retinopathy. *Arch Ophthalmol*. 1963;70:474–481.
52. Zhang Q, Presswalla F, Calton M, et al. Highly differentiated human fetal RPE cultures are resistant to the accumulation and toxicity of lipofuscin-like material. *Invest Ophthalmol Vis Sci*. 2019;60:3468–3479.
53. Feeney L. Lipofuscin and melanin of human retinal pigment epithelium. Fluorescence, enzyme cytochemical, and ultrastructural studies. *Invest Ophthalmol Vis Sci*. 1978;17:583–600.
54. Sparrow JR, Gregory-Roberts E, Yamamoto K, et al. The bisretinoids of retinal pigment epithelium. *Prog Retin Eye Res*. 2012;31:121–135.
55. Ach T, Huisingh C, McGwin G, et al. Quantitative autofluorescence and cell density maps of the human retinal pigment epithelium. *Invest Ophthalmol Vis Sci*. 2014;55:4832–4841.
56. Kevany BM, Palczewski K. Phagocytosis of retinal rod and cone photoreceptors. *Physiology*. 2010;25:8–15.
57. Katz ML, Robison Jr WG. What is lipofuscin? Defining characteristics and differentiation from other autofluorescent lysosomal storage bodies. *Arch Gerontol Geriatr*. 2002;34:169–184.
58. Delori FC, Goger DG, Dorey CK. Age-related accumulation and spatial distribution of lipofuscin in RPE of normal subjects. *Invest Ophthalmol Vis Sci*. 2001;42:1855–1866.
59. Curcio C, Millican CL, Allen K, Kalina R. Aging of the human photoreceptor mosaic: evidence for selective vulnerability of rods in central retina. *Invest Ophthalmol Vis Sci*. 1993;34:3278–3296.
60. Freund KB, Mrejen S, Jung J, Yannuzzi LA, Boon CJ. Increased fundus autofluorescence related to outer retinal disruption. *JAMA Ophthalmology*. 2013;131:1645–1649.
61. Zanzottera EC, Ach T, Huisingh C, Messinger JD, Freund KB, Curcio CA. Visualizing retinal pigment epithelium phenotypes in the transition to atrophy in neovascular age-related macular degeneration. *Retina (Philadelphia, Pa)*. 2016;36:S26.
62. Kellner U, Kraus H, Foerster M. Multifocal ERG in chloroquine retinopathy: regional variance of retinal dysfunction. *Graefe's Arch Clin Exp Ophthalmol*. 2000;238:94–97.
63. Allahdina AM, Stetson PF, Vitale S, et al. Optical coherence tomography minimum intensity as an objective measure for the detection of hydroxychloroquine toxicity. *Invest Ophthalmol Vis Sci*. 2018;59:1953–1963.
64. Allahdina AM, Chen KG, Alvarez JA, Wong WT, Chew EY, Cukras CA. Longitudinal changes in eyes with hydroxychloroquine retinal toxicity. *Retina*. 2019;39:473–484.
65. Kahn JB, Haberman ID, Reddy S. Spectral-domain optical coherence tomography as a screening technique for chloroquine and hydroxychloroquine retinal toxicity. *Ophthalmic Surg Lasers Imaging Retina*. 2011;42:493–497.
66. Curcio CA, Sloan KR, Kalina RE, Hendrickson AE. Human photoreceptor topography. *J Comp Neurol*. 1990;292:497–523.
67. Rodriguez-Padilla JA, Hedges TR, Monson B, et al. High-speed ultra–high-resolution optical

coherence tomography findings in hydroxychloroquine retinopathy. *Arch Ophthalmol*. 2007;125:775–780.
68. Marmor MF, Hu J. Effect of disease stage on progression of hydroxychloroquine retinopathy. *JAMA Ophthalmol*. 2014;132:1105–1112.
69. Garrity ST, Jung JY, Zambrowski O, et al. Early hydroxychloroquine retinopathy: optical coherence tomography abnormalities preceding Humphrey visual field defects. *Br J Ophthalmol*. 2019;103:1600–1604.
70. Solberg Y, Dysli C, Möller B, Wolf S, Zinkernagel MS. Fluorescence Lifetimes in Patients With Hydroxychloroquine Retinopathy. *Invest Ophthalmol Vis Sci*. 2019;60:2165–2172.
71. Reiter GS, Told R, Schlanitz FG, et al. Impact of drusen volume on quantitative fundus autofluorescence in early and intermediate age-related macular degeneration. *Invest Ophthalmol Vis Sci*. 2019;60:1937–1942.